

Gaussian State Description of Squeezed Light

Vivi Petersen,^{1,2} Lars Bojer Madsen,² and Klaus Mølmer^{1,2}

¹*QUANTOP - Danish National Research Foundation Center for Quantum Optics*

²*Department of Physics and Astronomy, University of Aarhus, DK-8000 Århus C, Denmark*

(Dated: December 27, 2018)

We present a Gaussian state description of squeezed light generated in an optical parametric oscillator. Using the Gaussian state description we describe the dynamics of the system conditioned on homodyne detection on the output field. Our theory shows that the output field is squeezed only if observed for long enough times or by a detector with finite bandwidth. As an application of the present approach we consider the use of finite bandwidth squeezed light together with a sample of spin-polarized atoms to estimate a magnetic field.

PACS numbers: 42.50.Dv,03.67.Mn,03.65.Ta,07.55.Ge

I. INTRODUCTION

Quantum mechanical squeezing of optical fields represents a means to improve precision measurements below the standard quantum noise limit for optical detection. These measurements exercise a significant back-action on the probed system, and to assess the achievement of a detection scheme we need a formalism that can deal with light-matter interaction and measurement induced state reduction continuously in time. Now, a continuous wave beam of light is described by infinitely many modes, for example in time or frequency domain, and the quantum state of the light field and of the system interacting with the beam is in general too complicated to be fully accounted for in a Schrödinger picture representation. In many quantum optical problems with constant or periodic driving Hamiltonians, it has been possible, however, to provide solutions in the Heisenberg picture for the relationship between Fourier transformed frequency components of the field and system observables. Unfortunately this well-established technique does not apply in conjunction with measurements on the joint system acting locally in time and hence affecting all frequency components of the observables at each measurement event. The present paper does not provide a solution to this general problem. Instead, we shall demonstrate that for a specific dynamics restricted to a specific class of states, the so-called Gaussian states, a significant reduction in the number of parameters needed to fully characterize the system enables a complete description. The squeezed light produced in an optical parametric oscillator (OPO) is in such a Gaussian state, implying that the field is fully characterized by the first-order and second-order correlation functions of the field variables. The interaction with an atomic system may destroy the Gaussian character, but we shall restrict our attention to optical interaction with a large collection of atoms through an effective collective atomic observable, which may in turn be well described by a Gaussian quantum state. The Gaussian state formalism [1, 2, 3] was recently employed [4, 5, 6] for the off-resonant Faraday rotation-like interaction between a continuous beam of light and an atomic ensemble. To

describe the interaction with a continuous wave of light, we proposed [4, 5, 6] to treat the beam as a sequence of short segments of light incident on the atoms. In the interaction, each light segment acquires some entanglement with the atomic sample and causes a modification of the atomic state when the light segment is probed after the interaction. The description of the incident optical beam is simple if the state of the field factorizes in components corresponding to each short segment of the beam. This is indeed the case for a coherent state of light, representing a normal laser beam. Realistic sources of squeezed light, on the other hand, have a finite bandwidth of squeezing which implies that correlations exist between the field observables at different times. Here, we extend the Gaussian formalism to the case of the continuous output from an optical parametric oscillator (OPO). We reproduce the properties of the squeezed optical beam which are already known from standard quantum optics treatments, and we apply our formalism to the example of atomic magnetometry.

The paper is organized as follows. In Sec. II, we recall some results of the standard treatment of squeezing in an OPO. In Sec. III, we present the Gaussian state description of this system. In Sec. IV, we turn to magnetometry. The Larmor precession of an atomic sample caused by an unknown magnetic field is probed by optical Faraday rotation, and the value of the magnetic field is gradually determined as measurement data are accumulated. The use of a squeezed light source improves the magnetometer for probing times larger than the inverse bandwidth of squeezing. In Sec. V, we conclude.

II. GENERATION OF SQUEEZED LIGHT IN AN OPTICAL PARAMETRIC OSCILLATOR

In this section, we present a simple model of squeezed light generation in a cavity with a non-linear medium which is pumped by a classical pump beam at frequency $2\omega_c$, twice the cavity resonance frequency, and giving rise to creation and annihilation of pairs of photons by the

Hamiltonian [7] (we use $\hbar = 1$ throughout)

$$\mathcal{H}_{\text{int}} = ig(a^{\dagger 2} - a^2) = g(x_c p_c + p_c x_c) \quad (1)$$

where a^\dagger and a are the creation and annihilation operators for the light inside the cavity, and where the canonical conjugate variables are

$$\begin{aligned} x_c &= \frac{1}{\sqrt{2}}(a + a^\dagger) \\ p_c &= \frac{1}{i\sqrt{2}}(a - a^\dagger). \end{aligned} \quad (2)$$

We express the Hamiltonian in a frame rotating with the cavity resonance frequency ω_c , and consider the dynamics in this rotating frame.

In the absence of losses, the Heisenberg equations of motion

$$\begin{aligned} \dot{x}_c(t) &= 2gx_c(t) \\ \dot{p}_c(t) &= -2gp_c(t) \end{aligned} \quad (3)$$

can be solved straightforwardly, leading to an exponential squeezing of the p_c -variable and an accompanying anti-squeezing of the x_c -variable, which maintains a constant value of the uncertainty product.

This model produces a squeezed state of a single light mode inside the cavity, and such states are subject to detailed analysis in most text books on quantum optics. Here, however, we aim at applications of squeezed light and hence we are interested in the squeezing properties of the light that leaks out of the cavity. This light propagates out of the cavity into a continuous beam, which corresponds to a continuum of modes in frequency space. We thus replace one of the perfectly reflecting cavity mirrors with a mirror with a small transmittance, which will lead to a loss of the cavity field with rate Γ . The resulting intra-cavity field state can be found in many different ways, but for our purpose it is sufficient to note that the cavity mirror acts as a beam splitter for the intra-cavity field and for the vacuum field ($x_{\text{ph,in}}, p_{\text{ph,in}}$) incident on the cavity, see Fig. 1. At the partly transmitting mirror the incident field is reflected into the output field. The output field is a linear combination of the reflected incident field and the transmitted intra-cavity field. Imagine an incident beam segment of duration τ , short enough that the intensity transmitted at the mirror and the field amplitude built up by the Hamiltonian (1) can be treated to lowest order in τ . We can then iterate the Heisenberg equations of motion for the intra-cavity field and the output field from the cavity and we obtain

$$x_c(t + \tau) = (\xi + 2g\tau)x_c(t) + \sqrt{\Gamma\tau}x_{\text{ph,in}}(t) \quad (4a)$$

$$p_c(t + \tau) = (\xi - 2g\tau)p_c(t) + \sqrt{\Gamma\tau}p_{\text{ph,in}}(t) \quad (4b)$$

$$x_{\text{ph,out}}(t + \tau) = -\sqrt{\Gamma\tau}x_c(t) + \xi x_{\text{ph,in}}(t) \quad (4c)$$

$$p_{\text{ph,out}}(t + \tau) = -\sqrt{\Gamma\tau}p_c(t) + \xi p_{\text{ph,in}}(t). \quad (4d)$$

where $\xi^2 = 1 - \Gamma\tau$ denotes the probability for the segment to be reflected by the mirror. This quantity is very

close to unity, and consequently $\xi \approx 1 - \Gamma\tau/2$. The expressions (4a–4d) are of course equivalent to the ones obtained by the conventional input-output formalism [8, 9], with the last terms in (4a,4b) having the characteristic properties of Wiener noise increments in the limit of small τ . Since we assume that the input field is in the vacuum state, Eqs. (4a,4b) can be solved directly for the variances of the intra-cavity field quadratures, starting from the vacuum at $t = 0$, and taking the $\tau \rightarrow 0$ limit

$$\text{Var}(x_c) = \frac{1}{2} \frac{\Gamma - 4ge^{-(\Gamma-4g)t}}{\Gamma - 4g} \quad (5)$$

$$\text{Var}(p_c) = \frac{1}{2} \frac{\Gamma + 4ge^{-(\Gamma+4g)t}}{\Gamma + 4g}. \quad (6)$$

If $4g < \Gamma$, we see that these equations approach steady state for large times t . Since we are interested in operating the OPO in a regime where steady state can be obtained, we assume from now on that $4g < \Gamma$. The light inside the cavity is still squeezed as expected, but it is entangled with the emitted light, and hence it is not in a pure state and also not in a minimum uncertainty state.

In the conventional input-output description, by a Fourier transformation to frequency space, the equations (4) become algebraic equations, and the output field operators in frequency space are expressed as linear combinations of the input operators at the same frequencies but with frequency dependent coefficients [10]. All moments of the field annihilation and creation operators have trivial expectation values in the vacuum state. If ω denotes the difference between the optical frequency and the cavity resonance frequency ω_c , we have for example the following expression for the normal ordered expectation value of the output field when the system has reached steady state (remembering $4g < \Gamma$)

$$\langle : x(\omega), x(\omega') : \rangle = \frac{2\Gamma g}{(\frac{\Gamma}{2} - 2g)^2 + \omega^2} \delta(\omega + \omega'). \quad (7)$$

The Lorentzian frequency dependence implies a temporal correlation between the light emitted at different times, which is due to the common origin in the intra-cavity field. The field at a single instance of time is obtained by a Fourier transformation of the expressions in frequency space. This will involve all frequencies, also the ones far from the cavity resonance and hence outside the bandwidth of squeezing. Consequently, one will not observe squeezing properties if one observes a light field in a time interval shorter than $\sim 1/\Gamma$. Integrating the signal over a finite time interval T , corresponding to detection of the variable

$$x_T = \frac{1}{\sqrt{T}} \int_t^{t+T} x(t') dt' \quad (8)$$

yields a quantity with normal ordered expectation value

$$\begin{aligned} \langle : x_T^2 : \rangle &= \frac{1}{2T} \int_0^T \int_0^T : x(t)x(t') : dt dt' \\ &= \frac{1}{4\pi T} \int_0^T \int_0^T \int_{-\infty}^{\infty} \int_{-\infty}^{\infty} : x(\omega)x(\omega') : \\ &\quad e^{-i\omega t} e^{-i\omega' t} d\omega d\omega' dt dt' \\ &= \frac{8g\Gamma}{T(\Gamma - 4g)^3} \left[(\Gamma - 4g)T - 2 + 2e^{(-\Gamma/2+2g)T} \right]. \end{aligned} \quad (9)$$

If we use that $\langle x_T^2 \rangle = \langle : x_T^2 : \rangle + 1/2$ we see that for short times $((\Gamma - 4g)T \ll 1)$, the output field has the standard noise of vacuum, whereas integration over a longer time interval yields

$$\text{Var}(x_T) \rightarrow \frac{1}{2} \frac{(\Gamma + 4g)^2}{(\Gamma - 4g)^2}. \quad (10)$$

The corresponding variance for the p_T component is obtained by replacing g by $-g$ in the above expressions, i.e., in the long-time limit the emitted field is described by a minimum uncertainty state.

The prediction of the noise properties of x_T and p_T should of course be in agreement with the ones observed if one carries out a homodyne measurement to detect these quantities, but it is important to remember that during such detection, the dynamics of the system will be different, and it is not clear how to modify the relations in frequency space between the intra-cavity and output fields as the detection takes place in real time.

In the next section, we introduce the Gaussian state formalism which allows an effective real-time treatment of the production *and* probing of squeezed light.

III. GAUSSIAN STATES

A. General Formalism

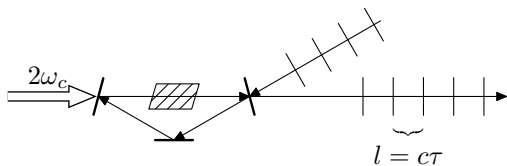


FIG. 1: Generation of squeezed light by an optical parametric process pumped by a classical field at $2\omega_c$. The figure shows three field segments in the vacuum state which enter the cavity, where a non-linear medium generates squeezing. Four segments of light are shown propagating away from the cavity.

The linear transformation between the states of the cavity field and a segment of light initially incident on the cavity, and eventually propagating away from the

cavity (4) is easy to deal with, because a state which is initially Gaussian in the field variables will remain Gaussian at later times. Taking an initially empty cavity and the incident vacuum field, will hence lead to Gaussian states at all later times. We want to consider the continuous emission of light by the cavity, and we therefore imagine one segment of light after the other leaving the cavity, see Fig. 1, and all field quadratures being given by a multi-mode Gaussian distribution. A Gaussian state is fully characterized by the mean value vector of all canonical variables, which we arrange in a column vector \mathbf{y} , with $\mathbf{m} = \langle \mathbf{y} \rangle$ and the covariance matrix γ where $\gamma_{ij} = 2\text{Re}(\langle (y_i - \langle y_i \rangle)(y_j - \langle y_j \rangle) \rangle)$. If the output field is discretized in N segments \mathbf{m} has dimension $(2N + 2)$ with $2N$ effective x and p variables for the output field and 2 variables, x_c, p_c , for the cavity mode. The covariance matrix γ has dimension $(2N + 2) \times (2N + 2)$. These finite objects are of course far easier to deal with than the full $N + 1$ tensor products of infinite dimensional Hilbert spaces. In practice the formalism can be made even simpler if we assume that the output beam is detected right after it is emitted from the cavity, and hence the quantum state of each light beam segment is destroyed and only the classical output value is retained, while the next segment emerges from the cavity. Let us consider the interaction between a single incident segment of light and the intra-cavity field, and let us write the linear transformation of the four field variables $\mathbf{y} = (x_c, p_c, x_{\text{ph}}, p_{\text{ph}})^T$ as follows

$$\mathbf{y} \mapsto \mathbf{S}\mathbf{y} \quad (11)$$

where the elements of the 4×4 matrix \mathbf{S} follow directly from the transformation (4). Under this transformation, the mean value vector \mathbf{m} and the covariance matrix γ transform as

$$\mathbf{m}(t + \tau) = \mathbf{S}\mathbf{m}(t) \quad (12)$$

$$\gamma(t + \tau) = \mathbf{S}\gamma(t)\mathbf{S}^T. \quad (13)$$

We write the 4×4 covariance matrix as

$$\gamma = \begin{pmatrix} \mathbf{A}_\gamma & \mathbf{C}_\gamma \\ \mathbf{C}_\gamma^T & \mathbf{B}_\gamma \end{pmatrix} \quad (14)$$

where \mathbf{A}_γ is the covariance matrix for the intra-cavity field variables, \mathbf{B}_γ is the covariance matrix for the beam segment in the continuous beam, and \mathbf{C}_γ represents their mutual correlations. An advantage of the Gaussian description is that the back-action on the residual system due to measurement may be accounted for explicitly. If we measure the variable x_{ph} , due to their mutual correlation, we learn something about the intra-cavity x_c variable, i.e., its variance decreases, and simultaneously, to fulfill Heisenberg's uncertainty relation, $\text{Var}(p_c)$ increases. Following Refs. [1, 2, 3], we have the explicit update formula for the intra-cavity field covariance matrix after homodyne detection on the beam segment

$$\mathbf{A}_\gamma \mapsto \mathbf{A}_\gamma - \mathbf{C}_\gamma(\pi\mathbf{B}_\gamma\pi)^{-1}\mathbf{C}_\gamma, \quad (15)$$

where $\pi = \text{diag}(1, 0)$, and $()^-$ denotes the Moore-Penrose pseudoinverse. This result does not depend on the actual outcome of the measurement. The latter however, affects the mean values of the intra-cavity field variables. The beam segment has disappeared from the treatment, but to treat the interaction with the next segment we build the covariance matrix (14) describing the intra-cavity field and this new segment with

$$\mathbf{B}_\gamma \mapsto \mathbb{1} \quad (16)$$

$$\mathbf{C}_\gamma \mapsto 0, \quad (17)$$

corresponding to an incident vacuum state with no correlation with the cavity field yet. We propagate the system according to Eq. (13), and we implement the effect of the subsequent measurement by Eq. (15). The continuous production and probing of the beam is obtained by repetition of the above steps, and we may, in the limit of small time increments, derive a differential equation for the intra-cavity field \mathbf{A}_γ . This differential equation is of the general non-linear matrix Riccati form (see, e.g., Ref. [11] and references therein)

$$\dot{\mathbf{A}}_\gamma(t) = \mathbf{G} - \mathbf{D}\mathbf{A}_\gamma(t) - \mathbf{A}_\gamma(t)\mathbf{E} - \mathbf{A}_\gamma(t)\mathbf{F}\mathbf{A}_\gamma(t), \quad (18)$$

where the 2×2 matrices \mathbf{G} , \mathbf{D} , \mathbf{E} , \mathbf{F} are all derived from the expressions (13) and (15). As shown in Ref. [11] the solution for \mathbf{A}_γ can be expressed in terms of the solutions of two coupled linear matrix equations: $\mathbf{A}_\gamma = \mathbf{W}\mathbf{U}^{-1}$, where $\dot{\mathbf{W}} = -\mathbf{D}\mathbf{W} + \mathbf{G}\mathbf{U}$ and $\dot{\mathbf{U}} = \mathbf{F}\mathbf{W} + \mathbf{E}\mathbf{U}$.

B. Squeezing properties of the intra-cavity field

Applying the above general formalism to the squeezed light problem, we derive the Riccati equation (18) for the intra-cavity field covariance matrix, conditioned on the homodyne detection of the output field, and find the following matrices

$$\begin{aligned} \mathbf{G} &= \begin{pmatrix} 0 & 0 \\ 0 & \Gamma \end{pmatrix} \\ \mathbf{F} &= \begin{pmatrix} \Gamma & 0 \\ 0 & 0 \end{pmatrix} \\ \mathbf{D} &= \begin{pmatrix} -2g - \Gamma/2 & 0 \\ 0 & 2g + \Gamma/2 \end{pmatrix} \\ \mathbf{E} &= \mathbf{D}. \end{aligned} \quad (19)$$

Without detection, the beam and the intra-cavity field are entangled, and, as we noted above, the intra-cavity field state, regarded as a trace over the unobserved emitted field degrees of freedom is a mixed state and not a minimum uncertainty state. If we perform homodyne detection on the emitted field we find the same variance of x_c as above, but the variance of p_c changes to the value

$$\text{Var}(p_c) = \frac{1}{2} \frac{\Gamma - 4g}{\Gamma - 4ge^{-(\Gamma-4g)t}}. \quad (20)$$

In this case $\text{Var}(x_c) \cdot \text{Var}(p_c) = 1/4$ and we have a minimum uncertainty state of the intra-cavity field at all

times. If $4g < \Gamma$, we reach steady state for large times, and the variances then read

$$\text{Var}(x_c) = \frac{1}{2} \frac{\Gamma}{\Gamma - 4g} \quad (21)$$

$$\text{Var}(p_c) = \frac{1}{2} \frac{\Gamma - 4g}{\Gamma}. \quad (22)$$

In Fig. 2, we show how the variance of the Gaussian variables inside the cavity depends on time both with and without measurements on the output beam.

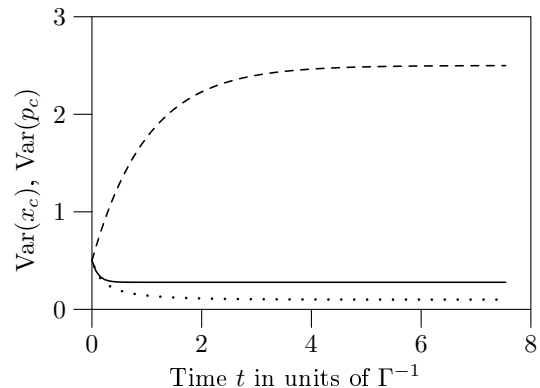


FIG. 2: Variances of the cavity variables x_c and p_c as a function of time. We use $\Gamma = 2\pi \times 6 \times 10^6 \text{ s}^{-1}$ and $g = 0.2\Gamma$ which are realistic experimental parameters for OPO's [12]. The variances of x_c with and without homodyne detection of the x_{ph} variable of the output field are identical and shown by the upper dashed curve. The full and the dotted curves show the variances of p_c without and with homodyne detection of the output field, respectively.

C. Squeezing properties of the emitted beam

1. Collective observable for many light segments

We now turn to the squeezing of the output beam. As discussed in Sec. II, there is no squeezing if we only consider small time intervals. To study the correlations between different individual segments we define the following collective operators

$$\begin{aligned} x_T &= \frac{1}{\sqrt{N}} \sum_{i=1}^N x_{\text{ph}_i}, \\ p_T &= \frac{1}{\sqrt{N}} \sum_{i=1}^N p_{\text{ph}_i}, \end{aligned} \quad (23)$$

where $T = \tau N$ is the accumulated time in N segments each of duration τ and where the field variables of the i^{th} segment are retained in the formalism. In appendix A, we calculate the variances of these quantities. The result

is given in Eq. (A13) and reads

$$\text{Var}(x_T) = \frac{1}{2T(\Gamma - 4g)^3} \left[(\Gamma - 4g)(\Gamma + 4g)^2 T - 32\Gamma g + 32\Gamma g e^{(-\Gamma/2+2g)T} \right]. \quad (24)$$

The result for $\text{Var}(p_T)$ is obtained by replacing g with $-g$. If we let $T \rightarrow 0$, we obtain $\text{Var}(p_T) = \frac{1}{2}$ showing that there is no squeezing if we only consider short times. If, on the other hand, we let $T \rightarrow \infty$, we obtain

$$\text{Var}(x_T) \rightarrow \frac{1}{2} \frac{(\Gamma + 4g)^2}{(\Gamma - 4g)^2}. \quad (25)$$

These results are in full agreement with the ones obtained by the usual quantum optics treatment discussed in Sec. II (see Eq. (10)).

2. Finite Bandwidth Detection

An alternative way to extract the squeezed component of the emitted beam, is to use a frequency filter, that selects the frequency range of interest. The modelling of such a detector involves a second cavity, in which the light segments enter and the intra-cavity field in the second cavity builds up. The squeezed beam contains photons in the relevant frequency band, but not only intensity builds up in the detecting cavity, we also expect the intra-cavity field to show squeezing properties. The variables used in

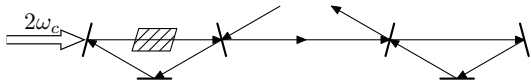


FIG. 3: Proposed setup for the characterization of the spectrum of squeezed light from an OPO (to the left). The squeezing properties of the single-mode field accumulated in the frequency tunable cavity to the right are determined (see text).

a Gaussian treatment of this problem, corresponding to the two cavity fields and the propagating beam segment, are $\mathbf{y} = (x_{c_1}, p_{c_1}, x_{c_2}, p_{c_2}, x_{\text{ph}}, p_{\text{ph}})$ and the Heisenberg equations of motion are obtained by a simple extension of the expressions used already in the case of a single cavity, where we replace Γ with Γ_1 . The second cavity is used to model the finite bandwidth detection. It has a decay constant Γ_2 and a tunable cavity resonance frequency $\omega_c + \delta$. In our frame rotating at ω_c the field variables in the second cavity obey the equations

$$x_{c_2}(t + \tau) = (1 - \Gamma_2\tau/2)x_{c_2}(t) + i\delta\tau p_{c_2}(t) + \sqrt{\Gamma_2\tau}x_{\text{ph,out}}(t) \quad (26)$$

$$p_{c_2}(t + \tau) = (1 - \Gamma_2\tau/2)p_{c_2}(t) - i\delta\tau x_{c_2}(t) + \sqrt{\Gamma_2\tau}p_{\text{ph,out}}(t) \quad (27)$$

where $x_{\text{ph,out}}, p_{\text{ph,out}}$ are the quadrature variables for the field leaving the first cavity, cf., Eqs. (4c,4d). In

Eqs. (26,27) the field incident on the second cavity is the output field from the first cavity, cf. Fig. 3. Due to the physical separation L of the two cavities and the finite speed of light the field variables in Eqs. (4c,4d) should in fact have been delayed by L/c , but since we are addressing the steady state properties of the system we can solve Eqs. (4c,4d) with the same time arguments. The output field from the second cavity is described by equations similar to Eqs. (4c,4d), but they will not be needed in the following. The detuning δ of the second cavity can be scanned, and the squeezing parameter of the intra-cavity variables x_{c_2}, p_{c_2} reflect the spectral properties of the output beam from the first cavity.

Fig. 4 shows the eigenvalues V_{\min} and V_{\max} of the 2×2 covariance matrix for the probing cavity as function of the detuning with respect to ω_c . In panel 4(a) the probing cavity has a damping rate Γ_2 comparable with the one of the OPO cavity, i.e., the intra-cavity field builds up with a memory time shorter than the time needed to see the full effect of squeezing. In panel 4(b), we use a detector system with narrow bandwidth, the cavity builds up light over a longer time interval, and the degree of squeezing is clearly larger than in 4(a). The Riccati equation can be solved analytically, and for $\delta = 0$ we obtain

$$V_{\max} = \frac{1}{2} \frac{(\Gamma_1 + 4g)^2 + (\Gamma_1 - 4g)\Gamma_2}{(\Gamma_1 - 4g)(\Gamma_1 + \Gamma_2 - 4g)}. \quad (28)$$

Here V_{\min} is obtained from V_{\max} by replacing g with $-g$. The insert shows V_{\min} and V_{\max} as function of Γ_2 . For large Γ_2 , the second cavity is equally fed by a wide range of frequency components, and the variance is dominated by the vacuum uncertainty: $V_{\min} = V_{\max} = 1/2$. If $\Gamma_2 = 0$ we obtain

$$V_{\max} = \frac{1}{2} \frac{(\Gamma_1 + 4g)^2}{(\Gamma_1 - 4g)^2} \quad (29)$$

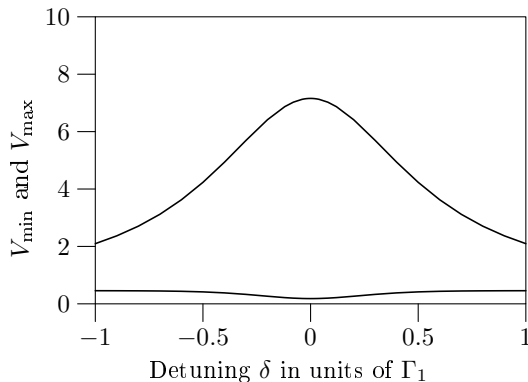
$$V_{\min} = \frac{1}{2} \frac{(\Gamma_1 - 4g)^2}{(\Gamma_1 + 4g)^2} \quad (30)$$

which equal the long-time integrated amplitudes (25).

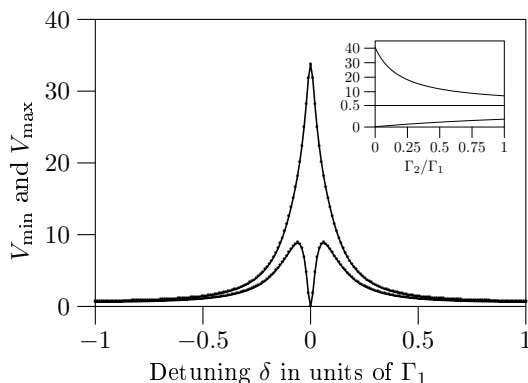
We note that the calculations here were significantly easier than in the case where we treated a large number of light segments simultaneously. This is because the mode of the second cavity in practice integrates the incident field over time and stores the contribution of many short beam segments in a single set of variables. We believe that this is a useful model of realistic finite bandwidth detectors, and that the approach can be used quite generally to investigate how finite optical bandwidth detection affects the sensitivity of metrology and the entanglement and spin squeezing of atomic samples.

IV. MAGNETOMETRY WITH SQUEEZED LIGHT

The purpose of introducing the Gaussian state formalism is to provide a theoretical approach, that allows a



(a)



(b)

FIG. 4: The variances V_{\min} and V_{\max} of the field inside the probing cavity as function of the detuning δ of this cavity with respect to ω_c in units of the decay width Γ_1 of the OPO cavity. We have used $\Gamma_1 = 2\pi \times 6 \times 10^6 \text{ s}^{-1}$ and $g = 0.2\Gamma_1$ as in Fig. 2. In (a) $\Gamma_2 = \Gamma_1$ and in (b) $\Gamma_2 = \Gamma_1/25$. The lower and upper parts of the insert in (b) show V_{\min} and V_{\max} respectively as functions of the bandwidth of detection Γ_2 for $\delta = 0$.

treatment of the interaction between light and an atomic sample in the regime where the quantum state of the atoms changes both because of the interaction itself and because the continuous measurements of the light field after the interaction teaches the observer about the state of the atoms. This measurement induced back-action on the quantum state of atoms plays a role in atomic magnetometry [13], it was used to spin squeeze atomic gasses [14] and to entangle pairs of gasses [15], and it recently played an important role in the realization of an atomic memory for light [16]. Since probing with squeezed light potentially is more precise, it was proposed in Ref. [4] that magnetometry would also benefit from the use of squeezed light, and a simple model with ultra-broad band squeezing indeed suggests improvement by precisely the squeezing factor on the B-field uncertainty. We will now

use magnetometry as an example to show how we can effectively treat the probing of atomic systems with a real squeezed optical field with finite bandwidth.

It is possible to estimate a magnetic field by a polarization rotation measurement of an off-resonant light beam passing through a trapped cloud of spin-1/2 atoms, see Fig. 5. All the atoms are assumed to be polarized with their spin along the x direction. We assume that the B-field component of interest is directed along the y direction, and hence it causes a Larmor rotation of the atomic spin toward the z axis. This in turn leads to a mean magnetization of the sample along the z direction, which will cause a Faraday rotation of the linear polarization of an optical field propagating through the sample. As the polarization rotation is proportional to the atomic spin component, and this is proportional to the B-field, the B-field estimated by the measurement is trivially obtained. We wish to address the error bar, i.e., the standard deviation on our estimate of the field as a function of the measurement record. The Gaussian state description which operates explicitly with the variances and covariance elements of the physical quantities is ideal for this analysis.

The gas of trapped spin-1/2 atoms is described by a collective spin operator $\mathbf{J} = (1/2) \sum_i \boldsymbol{\sigma}_i$ where $\boldsymbol{\sigma}_i$ are the Pauli spin matrices. The atoms are initially pumped such that they are polarized along the x axis and J_x can be treated as a classical variable $\langle J_x \rangle = N_{\text{at}}/2$ where N_{at} is the large number of atoms. The two other projections of the spin, J_y and J_z obey the commutation relation $[J_y, J_z] = iJ_x$ which may be rewritten as $[x_{\text{at}}, p_{\text{at}}] = i$ for the effective position and momentum variables $x_{\text{at}} = J_y/\sqrt{\langle J_x \rangle}$, $p_{\text{at}} = J_z/\sqrt{\langle J_x \rangle}$. The uncertainty is easily shown to be minimal in the initial state and, hence, the state pertaining to x_{at} and p_{at} is Gaussian.

Note that the OPO cavity produces a squeezed vacuum state; if this field is linearly polarized along the y -axis, it may be mixed on a polarizing beam splitter with a classical x polarized field to yield the field appropriate for polarization rotation measurements.

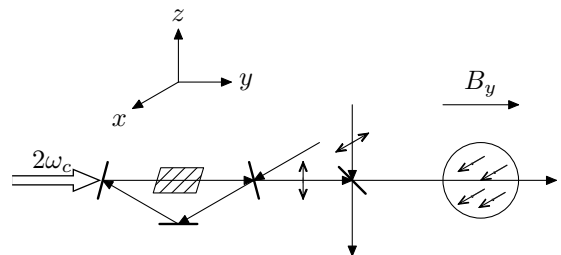


FIG. 5: Setup for estimating a B-field. In the cavity, we generate squeezed light which is linearly polarized along the z axis. We mix this field at an asymmetric beam splitter with a strong x polarized beam. The light then passes through a gas of polarized atoms, causing a rotation of the field polarization towards the z axis.

The light beam propagates along the y axis and is linearly polarized along x such that its Stokes operator

$\langle S_x \rangle = N_{\text{ph}}/2 = \Phi\tau/2$ is classical with N_{ph} the number of photons in a given segment of the beam and Φ is the photon flux. The two remaining Stokes vector components corresponding to the difference in photon numbers with linear polarization along directions at 45 and 135 degrees with respect to the x axis, and with left and right circular polarizations, respectively, have vanishing mean values, and they satisfy a commutator relation similar to the collective atomic spin. Accordingly, for the effective variables $x_{\text{ph}} = S_y/\sqrt{\langle S_x \rangle}$, $p_{\text{ph}} = S_z/\sqrt{\langle S_x \rangle}$, we have $[x_{\text{ph}}, p_{\text{ph}}] = i$ for $N_{\text{ph}} \gg 1$ and the initial coherent state of the field is a minimum uncertainty Gaussian state in these variables.

The effective Hamiltonian for this part of the system is

$$\mathcal{H}\tau = \kappa\sqrt{\tau}p_{\text{at}}p_{\text{ph}} + \mu\tau B_y x_{\text{at}}. \quad (31)$$

The characteristic atom-light coupling is $\kappa = \frac{d^2\omega}{\Delta A c \epsilon_0} \sqrt{2\langle J_x \rangle \Phi}$ where d is the atomic dipole moment, ω is the photon energy, Δ is the detuning of the light from atomic resonance, and A is the area of the light field. The coupling between the B-field and the atoms is $\mu = \beta\sqrt{\langle J_x \rangle}$ where β is the magnetic moment.

The classical B-field that we wish to estimate is treated as a random variable with a broad Gaussian probability distribution. Hence both the B-field, the atomic cloud, and the incident light pulse of duration τ are Gaussian variables. We arrange these in the vector $\mathbf{y} = (B_y, x_{\text{at}}, p_{\text{at}}, x_{\text{ph}}, p_{\text{ph}})^T$. The Larmor precession in time τ and the interaction between the atomic sample and the beam segment then leads to the linear transformation (11) of the variables [4, 6] given by

$$\mathbf{S} = \begin{pmatrix} 1 & 0 & 0 & 0 & 0 \\ 0 & 1 & 0 & 0 & \kappa\sqrt{\tau} \\ -\mu\tau & 0 & 1 & 0 & 0 \\ 0 & 0 & \kappa\sqrt{\tau} & 1 & 0 \\ 0 & 0 & 0 & 0 & 1 \end{pmatrix}. \quad (32)$$

The initial covariance matrix is $\gamma_0 = \text{diag}[2\text{Var}(B_0), 1, 1, 1, 1]$. After application of the matrix \mathbf{S} , and the operations (13) and (15) representing the polarization detection of the optical field, corresponding to a homodyne detection of the variable x_{ph} , the atomic variables and the B-field become correlated, a new beam segment enters in the standard coherent state as described by (16) and (17), and the evolution proceeds. In the limit of short beam segments, the evolution can be replaced by a Riccati differential equation for the 3×3 covariance matrix for the atoms and the B-field, and this equation can be solved analytically [4]. The variance of the B-field is

$$\text{Var}(B(t)) = \frac{\text{Var}(B_0)(\kappa^2 t + 1)}{\frac{1}{6}\kappa^4 \mu^2 \text{Var}(B_0)t^4 + \frac{2}{3}\kappa^2 \mu^2 \text{Var}(B_0)t^3 + \kappa^2 t + 1} \xrightarrow{t \rightarrow \infty} \frac{6}{\kappa^2 \mu^2 t^3} \propto \frac{1}{N_{\text{at}}^2 \Phi t^3} \quad (33)$$

which yields precisely the error on the estimate of the B-field. We note that the uncertainty of the field strength decreases as $1/(N_{\text{at}} t^{3/2})$ and not as $1/\sqrt{N_{\text{at}} t}$ as one might expect from standard counting statistics arguments. This improved precision is due to the squeezing of the atomic spin during the probing process.

A. Squeezed light

In Refs. [4] we modelled the use of squeezed light by introducing the squeezing parameter r such that Eq. (16) is replaced by

$$\mathbf{B}_\gamma \mapsto \begin{pmatrix} 1/r & 0 \\ 0 & r \end{pmatrix}, \quad (34)$$

i.e., every beam segment enters the interaction in a squeezed state. Going through the calculations we find that κ^2 should be replaced with $\kappa^2 r$ in Eq. (33): the B-field estimate is improved.

As noted in Ref. [4], this treatment of a squeezed beam, in the limit of small τ , is only valid if the squeezing bandwidth is infinite. The squeezing properties of the beam from an OPO, however, only reveal themselves if a narrow frequency component is selected, or if the field is integrated over times longer than the inverse bandwidth of squeezing, which are certainly longer than the infinitesimal τ employed in the continuous limit, where the Riccati equation is solved.

The full probing may well take longer than the inverse bandwidth, and one would hence expect that one still benefits from the squeezing in this longer time limit. We shall verify this assumption by a calculation in which we treat the probing with the field coming out of our OPO cavity in the full Gaussian formalism.

The example serves as a model for how to consider other atomic probing schemes with realistic squeezed light sources. We treat as Gaussian variables the B-field, the atomic variables, the intra-cavity field, and a single segment of light $\mathbf{y} = (B_z, x_{\text{at}}, p_{\text{at}}, x_c, p_c, x_{\text{ph}}, p_{\text{ph}})^T$. The beam segment enters on the cavity mirror in the vacuum state, it is reflected off the mirror with some squeezing and some entanglement with the partly transmitted intra-cavity field, it interacts with the atoms, and finally it is detected by homodyne detection, causing a moderate change of the joint covariance matrix for the B-field, the atoms, and the intra-cavity field. The transformation to lowest order in τ of the variables is now given by

$$\mathbf{S} = \begin{pmatrix} 1 & 0 & 0 & 0 & 0 & 0 & 0 \\ \mu\tau & 1 & 0 & 0 & 0 & 0 & 0 \\ 0 & 0 & 1 & \kappa\sqrt{\Gamma}\tau & 0 & -\kappa\sqrt{\tau} & 0 \\ 0 & 0 & 0 & \xi + 2g\tau & 0 & \sqrt{\Gamma}\tau & 0 \\ 0 & 0 & 0 & 0 & \xi - 2g\tau & 0 & \sqrt{\Gamma}\tau \\ 0 & 0 & 0 & -\sqrt{\Gamma}\tau & 0 & \xi & 0 \\ 0 & -\kappa\sqrt{\tau} & 0 & 0 & -\sqrt{\Gamma}\tau & 0 & \xi \end{pmatrix}, \quad (35)$$

with $\xi = 1 - \Gamma\tau/2$ as introduced in Eq. (4). Note that this matrix combines the elements present in the transformation of the field components alone (4) and the B-field-atom and light-atom interaction (32). Again the beam segment is inserted in its vacuum state (16), and it is probed by homodyne detection leading to the update formula (15). The bandwidth is taken care of by the intra-cavity field which establishes the necessary correlation between beam segments detected at different times. In the continuous limit we find the corresponding Riccati equation, and its solution provides the variance of the B-field as a function of time as shown in Fig. 6. The figure shows both the results without squeezing, with finite bandwidth squeezing, and the simple infinite bandwidth result (33) with a simple squeezing parameter r applied to each segment. We take the value $r = \frac{(\Gamma+4g)^2}{(\Gamma-4g)^2}$, corresponding to the long-time limit of Eq. (25), and we see a good agreement for long times between the two curves for squeezed states. We also see, that the finite bandwidth curve is an improvement with respect to the case of non-squeezed light, but that we have to probe for a certain time on the order of the squeezing bandwidth before we see the effect of squeezing. Indeed, the finite bandwidth curve is to a good approximation simply delayed by $16g \frac{3\Gamma+4g}{(\Gamma-4g)(\Gamma+4g)^2}$ compared with the infinite broad-band squeezed light curve.

The analytical result for $\text{Var}(B)$ is very lengthy. For small times t we get the result without squeezing as can be seen in Fig. 6, and for large t the result is exactly the same as in the infinite bandwidth case $\text{Var}(B(t)) = \frac{6}{\mu^2\tau\kappa^2t^3}$ if we identify the squeezing parameter by $r = \frac{(\Gamma+4g)^2}{(\Gamma-4g)^2}$.

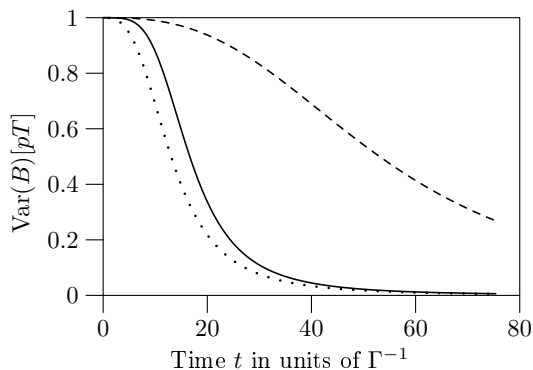


FIG. 6: Variance of the B field as a function of time. We use the same value of g and Γ as in Fig. 2, and $\kappa^2 = 1.83 \times 10^6 \text{ s}^{-1}$ and $\mu = 8.79 \times 10^4 (\text{s pT})^{-1}$. The dashed line is without squeezing, the full line is with squeezed light generated in a cavity, and the dotted line is with the squeezing parameter r .

V. CONCLUSION AND OUTLOOK

In summary, we have presented a Gaussian state description of the light from an optical parametric oscillator and its interaction with large atomic samples. The treatment is very effective, because the state of the parts of the beam that have just left the OPO cavity can be treated as a single mode, corresponding to a short beam segment, and after the interaction, the segment can be eliminated from the formalism. Here, we presented the dynamics when the field is probed by homodyne detection, and it is turned into classical information; if the beam propagates away without detection, it may be traced out of the formalism, which is an even simpler operation in the Gaussian formalism, since the corresponding rows and columns in the covariance matrix should just be removed. Finite bandwidth effects are included in the treatment by retaining the quantum state of the intra-cavity field, which is also a single field mode, i.e., at the price of adding a single pair of canonically conjugate variables (x_c, p_c) , which in the Gaussian formalism is done by adding two extra rows and columns to the covariance matrix.

The use of squeezed light holds the potential to improve spin squeezing, entanglement, and precision probing, and we demonstrated such an improvement in the case of magnetometry compared with the infinite bandwidth case, we also showed how the finite bandwidth of squeezing manifests itself as a time lag before the improvement is obtained in agreement with the observation that squeezing is only present in a light beam, if one integrates a sufficiently long part of the beam.

The method described is fully general, and further studies can be carried out along the same lines on other proposals involving squeezed light. It is readily generalized to incorporate more atomic systems, more field modes, non-degenerate OPOs, and as we showed also finite detection bandwidth can be modelled by the addition of auxiliary modes. Finite bandwidth of the light sources and of the detection system may also play non-trivial roles in conjunction with decay and decoherence which set an upper limit to the degree of entanglement obtained in gasses [17].

Finally we note that squeezed light has been proposed as an ingredient in various quantum information protocols, such as teleportation [18], as a source of heralded single photons [19, 20], as a resource in continuous variable quantum computing and error correction [21]. In many of these protocols, an elementary analysis is given in terms of single mode fields, where indeed, a full time and frequency dependent analysis would be more appropriate.

Acknowledgments

LBM is supported by the Danish Natural Science Research Council (Grant No. 21-03-0163).

APPENDIX A: SQUEEZING OF OUTPUT FIELD

To calculate the variance of x_T and p_T defined in Eq. (23) we use the Gaussian description.

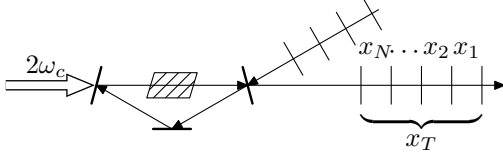


FIG. 7: The figure shows how we label the beam segments which are accumulated in x_T . We only obtain squeezing if we observe many beam segments, not if we only observe one segment.

The initial variables are $\mathbf{y}_1 = (x_c, p_c, x_{\text{ph}_1}, p_{\text{ph}_1})$ and the initial intra-cavity field and incident vacuum segment covariance matrix is

$$\gamma_1 = \begin{pmatrix} a_{11} & a_{12} & 0 & 0 \\ a_{12} & a_{22} & 0 & 0 \\ 0 & 0 & 1 & 0 \\ 0 & 0 & 0 & 1 \end{pmatrix}. \quad (\text{A1})$$

The associated transformation matrix is given by Eq. (4)

$$\mathbf{S}_1 = \begin{pmatrix} \xi + 2g\tau & 0 & \sqrt{\Gamma\tau} & 0 \\ 0 & \xi - 2g\tau & 0 & \sqrt{\Gamma\tau} \\ -\sqrt{\Gamma\tau} & 0 & \xi & 0 \\ 0 & -\sqrt{\Gamma\tau} & 0 & \xi \end{pmatrix}. \quad (\text{A2})$$

where $\xi = 1 - \Gamma\tau/2$ as introduced in Eq. (4). After the interaction $\tilde{\gamma}_1 = \mathbf{S}_1\gamma_1\mathbf{S}_1^T$. We now build the dynamics recursively by inserting two rows and columns between the second and third row and column in $\tilde{\gamma}$. In this way we represent the subsequent incident vacuum segments by

$$\gamma_{k+1} = \begin{pmatrix} \{\tilde{\gamma}_k\}_{(1:2,1:2)} & 0 & \{\tilde{\gamma}_k\}_{(1:2,3:2k+2)} \\ 0 & \mathbb{1}_{2 \times 2} & 0 \\ \{\tilde{\gamma}_k\}_{(3:2k+2,1:2)} & 0 & \{\tilde{\gamma}_k\}_{(3:2k+2,3:2k+2)} \end{pmatrix}. \quad (\text{A3})$$

The transformation matrix is

$$\mathbf{S}_k = \begin{pmatrix} \mathbf{S}_1 & 0 \\ 0 & \mathbb{1}_{(2k-2) \times (2k-2)} \end{pmatrix}, \quad (\text{A4})$$

and $\tilde{\gamma}_k = \mathbf{S}_k\gamma_k\mathbf{S}_k^T$. Eqs. (A4,A3) are now inserted, and the number of variables grows with time as we get more and more light segments, $\mathbf{y}_N = (x_c, p_c, x_{\text{ph}_N}, p_{\text{ph}_N}, \dots, x_{\text{ph}_1}, p_{\text{ph}_1})$

If $a_{12} = 0$ then every second element in γ is zero and γ can be rewritten on block diagonal form with similar x_{ph} and p_{ph} blocks. The system of equations for the x_{ph} , $\mathbf{y}_N = (x_c, x_{\text{ph}_1}, \dots, x_{\text{ph}_N})$, variables can be written as

$$\mathbf{S}_k = \begin{pmatrix} 1 - \Gamma\tau/2 + 2g\tau & \sqrt{\Gamma\tau} & 0 \\ -\sqrt{\Gamma\tau} & 1 - \Gamma\tau/2 & 0 \\ 0 & 0 & \mathbb{1}_{(k-1) \times (k-1)} \end{pmatrix} \quad (\text{A5})$$

$$\gamma_1 = \begin{pmatrix} a_{11} & 0 \\ 0 & 1 \end{pmatrix} \quad (\text{A6})$$

$$\gamma_k = \begin{pmatrix} A_k & 0 & \mathbf{C}_k \\ 0 & 1 & 0 \\ \mathbf{C}_k^T & 0 & \mathbf{B}_k \end{pmatrix} \quad (\text{A7})$$

where A_k is a real number, \mathbf{C}_k is a $1 \times (k-1)$ row vector, and \mathbf{B}_k is a $(k-1) \times (k-1)$ matrix.

From this we find the recurrence equations

$$A_{k+1} = (1 - \Gamma\tau/2 + 2g\tau)^2 A_k + \Gamma\tau \quad (\text{A8})$$

$$\mathbf{C}_{k+1}^T = \begin{pmatrix} -\sqrt{\Gamma\tau}(1 - \Gamma\tau/2 + 2g\tau)A_k + \sqrt{\Gamma\tau}(1 - \Gamma\tau/2) \\ (1 - \Gamma\tau/2 + 2g\tau)\mathbf{C}_k^T \end{pmatrix} \quad (\text{A9})$$

$$\mathbf{B}_{k+1} = \begin{pmatrix} \Gamma\tau A_k + (1 - \Gamma\tau/2)^2 & -\sqrt{\Gamma\tau}\mathbf{C}_k \\ -\sqrt{\Gamma\tau}\mathbf{C}_k^T & \mathbf{B}_k \end{pmatrix} \quad (\text{A10})$$

which can be solved, and the variance of x_T is found to be

$$\begin{aligned} \text{Var}(x_T) &= \frac{1}{N} \sum_{i=1}^N \sum_{j=1}^N \text{Cov}(x_i, x_j) \\ &= a_{11} \left[\frac{\Gamma\tau}{2N} \frac{1 - \alpha^{2N}}{1 - \alpha^2} \right. \\ &\quad \left. + \frac{\Gamma\tau\alpha^4}{N(1 - \alpha)} \left(\frac{1 - \alpha^N}{1 - \alpha} - \frac{1 - \alpha^{2N}}{1 - \alpha^2} \right) \right] \\ &\quad + \frac{\Gamma\tau^2}{2(1 - \alpha^N)} - \frac{\Gamma\tau^2}{2N} \frac{1 - \alpha^{2N}}{(1 - \alpha^2)^2} \\ &\quad + \frac{1}{2} (1 - \Gamma\tau/2)^2 - \Gamma\tau(1 - \Gamma\tau/2) \frac{1}{1 - \alpha} \\ &\quad + \frac{\Gamma\tau(1 - \Gamma\tau/2)}{N} \frac{1 - \alpha^N}{(1 - \alpha)^2} \\ &\quad + \frac{\Gamma\tau^2\alpha}{N(1 - \alpha^2)(1 - \alpha)} \left(N - \frac{1 - \alpha^N}{1 - \alpha} \right. \\ &\quad \left. + \alpha^3 \frac{1 - \alpha^{2N}}{1 - \alpha^2} - \alpha^3 \frac{1 - \alpha^N}{1 - \alpha} \right) \end{aligned} \quad (\text{A11})$$

where $\alpha = 1 - \Gamma\tau/2 + 2g\tau$. If we let $T = N\tau$ and then let $\tau \rightarrow 0$ then

$$\begin{aligned} \text{Var}(x_T) &\rightarrow \frac{1}{2T(\Gamma - 4g)^3} \left\{ (\Gamma - 4g)(\Gamma + 4g)^2 T \right. \\ &\quad - 4\Gamma(\Gamma + 8g) + 4a_{11}\Gamma(\Gamma - 4g) \\ &\quad - 8\Gamma[a_{11}(\Gamma - 4g) - (\Gamma + 4g)]e^{(-\Gamma/2+2g)T} \\ &\quad \left. - 4\Gamma[\Gamma - a_{11}(\Gamma - 4g)]e^{(-\Gamma+4g)T} \right\}. \end{aligned} \quad (\text{A12})$$

In the $T \rightarrow \infty$ limit, the first term dominates, and the expression for $\text{Var}(x_T)$ does not depend upon a_{11} .

In steady state we may insert $a_{11} = \frac{\Gamma}{\Gamma-4g}$ in Eq. (A12), and we obtain

$$\text{Var}(x_T) = \frac{1}{2T(\Gamma-4g)^3} \left[(\Gamma-4g)(\Gamma+4g)^2 T - 32\Gamma g + 32\Gamma g e^{(-\Gamma/2+2g)T} \right], \quad (\text{A13})$$

and

$$\text{Var}(p_T) = \frac{1}{2T(\Gamma+4g)^3} \left[(\Gamma+4g)(\Gamma-4g)^2 T - 32\Gamma g - 32g(\Gamma-4g)e^{-(\Gamma/2+2g)T} - 64g^2 e^{-(\Gamma+4g)T} \right]. \quad (\text{A14})$$

-
- [1] J. Fiurášek, Phys. Rev. Lett. **89**, 137904 (2002).
[2] G. Giedke and J. I. Cirac, Phys. Rev. A **66**, 032316 (2002).
[3] J. Eisert and M. B. Plenio, Int. J. Quant. Inf. **1**, 479 (2003).
[4] K. Mølmer and L. B. Madsen, Phys. Rev. A **70**, 052102 (2004).
[5] L. B. Madsen and K. Mølmer, Phys. Rev. A **70**, 052324 (2004).
[6] V. Petersen, L. B. Madsen, and K. Mølmer, Phys. Rev. A **71**, 012312 (2005).
[7] M. O. Scully and M. S. Zubairy, *Quantum Optics* (Cambridge University Press, 1997).
[8] M. J. Collett and C. W. Gardiner, Phys. Rev. A **30**, 1386 (1984).
[9] C. W. Gardiner, *Quantum Noise* (Springer, Berlin, Heidelberg, 1991).
[10] D. F. Walls and G. J. Milburn, *Quantum Optics* (Springer-Verlag, 1994).
[11] J. K. Stockton, J. M. Geremia, A. C. Doherty, and H. Mabuchi, Phys. Rev. A **69**, 032109 (2004).
[12] J. L. Sørensen, *Private communication*.
[13] J. M. Geremia, J. K. Stockton, A. C. Doherty, and H. Mabuchi, Phys. Rev. Lett. **91**, 250801 (2003).
[14] A. Kuzmich, L. Mandel, J. Janis, Y. E. Young, R. Eijnisman, and N. P. Bigelow, Phys. Rev. A **60**, 2346 (1999).
[15] B. Julsgaard, A. Kozhekin, and E. S. Polzik, Nature **413**, 400 (2001).
[16] B. Julsgaard, J. Sherson, J. I. Cirac, J. Fiurášek, and E. Polzik, Nature **432**, 482 (2004).
[17] J. Sherson and K. Mølmer, Phys. Rev. A **71**, 033813 (2005).
[18] A. Furusawa, J. L. Sørensen, S. L. Braunstein, C. A. Fuchs, H. J. Kimble, and E. S. Polzik, Science **282**, 706 (1998).
[19] C. K. Hong and L. Mandel, Phys. Rev. Lett. **56**, 58 (1986).
[20] C. R. Myers, M. Ericsson, and R. Laflamme, *A single photon source with linear optics and squeezed states*, quant-ph/0408194 (2004).
[21] S. L. Braunstein, Phys. Rev. Lett. **80**, 4084 (1998).